Journal of Alloys and Compounds 502 (2010) 451–455

Contents lists available at ScienceDirect

Journal of Alloys and Compounds

journal homepage: www.elsevier.com/locate/jallcom

Effect of substrate temperature on structural properties and corrosion resistance of carbon thin films used as bipolar plates in polymer electrolyte membrane fuel cells

A. Afshar[a], M. Yari[a,*], M.M. Larijani[b], M. Eshghabadi[a]

[a] Science and Research Branch, Islamic Azad University (IAU), Tehran, Iran
[b] Agricultural Medical and Industrial Research School, Nuclear Science and Technology Research Institute (NSTRI), Karaj, Iran

ARTICLE INFO

Article history:
Received 17 March 2010
Received in revised form 11 April 2010
Accepted 25 April 2010
Available online 5 May 2010

Keywords:
Thin films
Vapor deposition
Corrosion
Fuel cell
Stainless steel

ABSTRACT

In this work, the effects of substrate temperature that was changed from 100 to 500 °C on the structural, chemical and electrical properties of carbon films, prepared by direct current magnetron sputtering technique, on 316L stainless steel as bipolar plate had been investigated. Raman spectroscopy and scanning electron microscopy (SEM) were performed to study the structure and the morphology of the deposited films, respectively. The corrosion resistance and the electrical resistivity were carried out by using corrosion tests and four point-probe technique. The results show that the carbon films change the structure from amorphous to graphite-like by increasing temperatures. At the temperatures higher than 300 °C, the holes and porosities are formed on the film indicating a decrease of film quality. According to our results, corrosion resistance and electrical properties are depended strongly on the substrate temperature.

1. Introduction

Bipolar plates are multifunctional components in polymer electrolyte membrane fuel cells (PEMFCs). They account for about 45% of total stack cost and about 80% of total weight, which prevent PEMFCs from being widely used [1]. Traditionally, solid graphite is used for bipolar plates because of its low interfacial contact resistance and high corrosion resistance, but it is brittle, expensive to machine, and has poor cost effectiveness for mass production.

Metallic materials are candidates as bipolar plates because of their good mechanical strength, high gas impermeability, low cost and ease of manufacturing. Noble metals such as gold and palladium [2] and amorphous metals [3–5] are investigated. They have excellent performance in fuel cells. However, the high cost of these metals has prohibited their utilization for commercial use [6].

Inexpensive metals and alloys such as aluminum [7], stainless steel [8,9], nickel [10], copper [11], and titanium [12] could easily be processed into bipolar plates. Corrosion of the metallic bipolar plates leads to release of metal ions that can contaminate the electrolyte membrane, thus decrease membrane conductivity and efficiency of the fuel cell [13]. In addition, the formation of a passive, or oxide, or hydroxide layer on the metallic surface will increase the interfacial contact resistance by many orders of magnitude [13].

A possible solution is coating a conductive film on metallic bipolar plate to protect it against corrosion while keeping the contact resistance low. It seems that, carbon coating could significantly improve the corrosion resistance and the electrical conductivity. Indeed some attempts have been made to improve the performance of bipolar plates [14–20].

Fukutsuka et al. [14] prepared carbon coating on the 304 stainless steel by using plasma-assisted chemical vapor deposition. They concluded that the carbon coating on the 304 stainless steel might be a candidate technique for the improvement of metal bipolar plates. In another report, Show et al. [15,16] studied on the amorphous carbon (a-C) films deposited on titanium bipolar plate by radio frequency plasma enhanced chemical vapor deposition (RF-PECVD) method. They illustrated that using an a-C layer on metal bipolar plates improves the efficiency of fuel cells for electric power generation. After that, Chung et al. [17] used CVD process to deposit a carbon film on Ni-coated 304 stainless steel bipolar plates. They predicted that carbon-coated stainless steel plates may practically replace commercial graphite plates in the application of PEMFC. In a separate study [18], they also investigated on deposition of carbon film without Ni coating (catalyst layer). They believed that the use of such carbon-coated 304 stainless steel as bipolar plates is expected to reduce the volume while improving the performance of PEMFC. Fu et al. [19] tried to evaluate the effect of pure carbon,

* Corresponding author. Tel.: +98 2144869782; fax: +98 2144869784.
E-mail addresses: yari.m@srbiau.ac.ir, mehdi_yari@yahoo.com (M. Yari).

0925-8388/$ – see front matter © 2010 Elsevier B.V. All rights reserved.
doi:10.1016/j.jallcom.2010.04.194

C–Cr and C–Cr–N composite films on 316L stainless steel as bipolar plates. According to their results, C–Cr composite films satisfy the PEMFC recommendation more than the other kinds of coatings.

Here, we report on the structural, chemical stability and electrical properties of 316L stainless steel substrates coated by direct current magnetron sputtering PVD (MS-PVD). Also the effects of substrate temperature on the properties of studied films are discussed.

2. Materials and methods

The substrate material was 316L austenitic stainless steel. The chemical composition of the specimen is 16.4Cr–10.32Ni–1.94Mo–0.024C in %wt. The polished specimens were provided at an approximate size of 10 mm × 10 mm and 2 mm thickness. All the specimens were cleaned ultrasonically with ethanol and acetone prior to the coating treatments. The substrate temperature was increased with an electrical heater in range of 100–500 °C with ±5 °C tolerance. The MS-PVD chamber was pumped to a base pressure around 3×10^{-6} Pa and then high purity argon was flowed to reach the operating pressure around 4.3×10^{-5} Pa. The carbon plate with % 99.99 purity was used as the target. The distance between specimen and target was fixed at 4.5 cm. The plasma was applied by high voltage DC power source. Its voltage set at 800 V. For all samples the sputtering time was kept fixed at 8 min. During cooling down to 100 °C, the chamber was under argon atmosphere.

The carbon films were characterized by Raman spectroscopy method using a spectrometer of the type Labram HR800. Raman spectra were collected using 532 nm line from an Nd–YAG laser with a power of 10 mW. Morphology of the carbon coating was observed by scanning electron microscopy (SEM).

The corrosion resistance of the coated samples in 1 M H_2SO_4 with 5 ppm F^- ions at 70 ± 3 °C (i.e. simulated PEMFC solution) was evaluated by potentiodynamic polarization with potentiostat model 273A EG&G instruments. A saturated calomel electrode (SCE) was used as reference and a Pt rod served as the auxiliary electrode. The specimen was mounted in a fixture in order to avoid exposing uncoated area in contact of corrosion environment.

Polarization scan started at around −250 mV vs. open circuit potential (OCP) and continued in the anodic direction up to 0.9 mV vs. SCE with a potential scan rate of 1 mV s^{-1}.

There is a conventional method to measure interfacial contact resistance (ICR) [3–9,11,12] of the bipolar plates as PEMFC which is used by a majority of the researches. However, four point-probe instrument is also used by the others [15,16] to investigate the electrical properties of the films. In this work, the latter one (model Keithley) is applied for measuring the electrical resistivity. The voltage and current range were selected ±1 V and ±100 mA, respectively. It should be mentioned that, in order to reduce the reading errors, the probe and circuit resistances were subtracted from layer resistance (R_s). Considering R_s which is calculated from *I–V* characteristic curve, the sheet resistance (ρ) could be measured from the following equation:

$$\rho = \left(\frac{2\pi t}{\mathrm{Ln}\,2}\right) R_s \quad (1)$$

where *t* is the thickness of carbon films. The thickness of different films is measured by a profile-meter, Dektak 3 model, Version 2.13.

3. Results and discussion

Fig. 1 shows the Raman spectra of carbon films which were deposited at various temperatures. Each spectrum is mainly composed of two broad peaks at around 1600 and 1320 cm^{-1}. These peaks are named G-band and D-band, respectively. The G-band (graphite) is related to graphite lattice and sp^2 bands. The D-band (defect) results from the defects in the graphite crystalline structure. The intensity and width of D-band is proportional to the resonances of carbon atoms in disordered and defective graphite structure. The stronger intensity and the wide full width at half maximum (FWHM) of D-band denote an abundance of short range ordered graphite structures or graphite with very small grain size in the carbon film.

Table 1 summarizes the parameters extracted from Raman spectra in Fig. 1. FWHM and intensity for deconvoluted peaks were derived from the Lorentzian distribution fitting. Based on the fitting parameters, the ratio of the D and G intensity peaks (I_D/I_G) are determined. According to Fig. 2, the I_D/I_G ratio is increased abruptly by increasing the substrate temperature up to 300 °C, indicating the graphitization of films, and then is changed slightly above 400 °C. As reported in references [16,17,21–23], the shape of Raman spectra

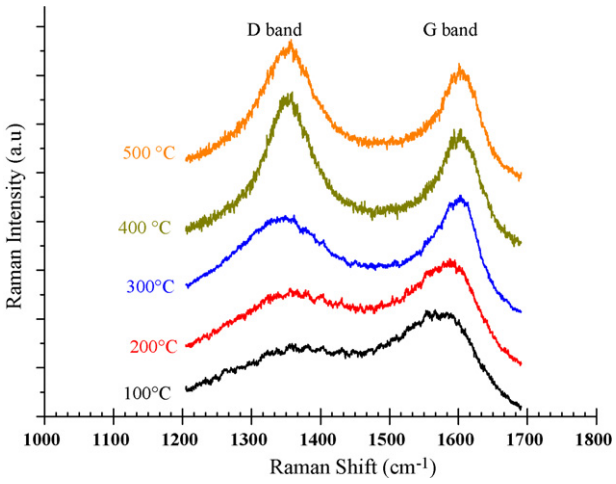

Fig. 1. Raman spectra of carbon films deposited at various substrate temperatures.

Table 1
Raman parameters extracted from Lorentzian deconvolution of Raman spectra in Fig. 1.

Substrate temperature (°C)	I_D/I_G	FWHM G (cm^{-1})	FWHM D (cm^{-1})
100	0.99	151	468
200	1.08	124	349
300	1.16	63	234
400	1.36	63	108
500	1.34	62	131

at 100 and 200 °C corresponds to the amorphous structure (a-C) of deposited carbon films. A further increasing of substrate temperature can change the a-C film microstructure towards graphitization due to the increase of carbon atom mobility and reduction of defect density as reported by Onoprienko et al. [21]. In agreement with Onoprienko et al., the transformation of distorted aromatic rings into regular ones occurs at temperature up to 400 °C (graphitization step). However, above 400 °C the growth mechanism changes with formation of graphite crystallites.

Fig. 3 shows FWHM of D and G bands as a function of substrate temperature. FWHM intensity for both D and G bands decreases with deposition temperature. D peak FWHM decreasing is more significant than G peak FWHM. Beeman et al. [24] believed that there is a relationship between D and G FWHM intensity in graphite and relaxation in the bond-angle distortion of the threefold coordinated carbon atoms towards an angle of 120°. By increasing deposition

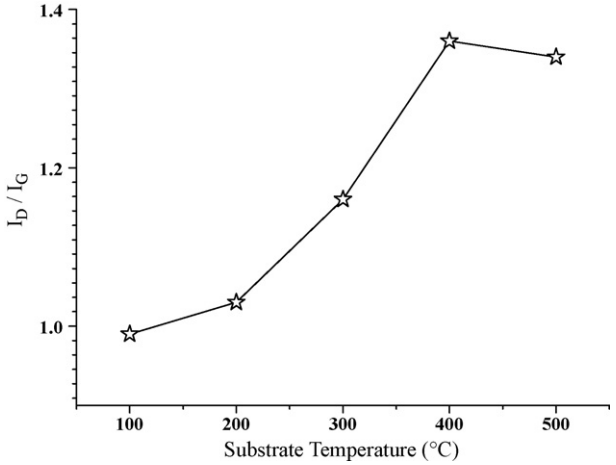

Fig. 2. Dependence of I_D/I_G ratio on deposition temperature.

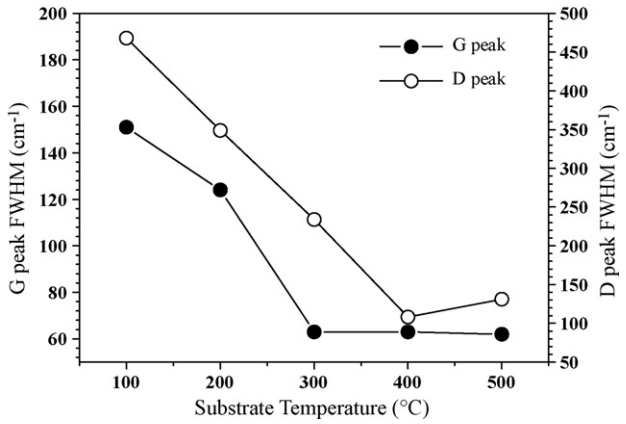

Fig. 3. FWHM of G and D peaks observed in Raman spectra of carbon films deposited at various temperatures.

temperature, atomic rearrangement processes causes relaxation of bond-angle distortions and therefore FWHM decreases by increasing temperatures. Cappelli et al. [22] declared that, narrowing D and G peaks (decrease in FWHM) by increasing temperature is related to temperature aggregation and ordering phenomenon due to atomic rearrangement processes.

When FWHM of the G peak exceeds 50 cm^{-1}, reveals that the size of graphite crystallites with sp^2 bands (L_a) is around or lower than 1 nm [25]. Ferrari and Robertson [26], showed that in this range of crystallite size, the I_D/I_G ratio can be related to L_a (in Angstrom) according to the following equation:

$$\frac{I_D}{I_G} = c.L_a^2 \quad (2)$$

which c is constant and equal to around 0.0055.

It is obvious from Table 1 that, the G peak FWHM is wider than 50 cm^{-1} for all samples. Therefore, we can approximately calculate the average of graphite grain size (L_a). L_a rises from 1.34 to 1.57 nm by increasing the substrate temperature. However the grain size of the crystallites is very small. We can classify deposited carbon films in amorphous and glassy carbon form [25].

Fig. 4 presents the potentiodynamic results for carbon-coated 316L stainless steel at various substrate temperatures. Extracted results from potentiodynamic curves are summarized in Table 2. According to Table 2, corrosion potential (E_{corr}) of the coated sample gradually increases up to 300 °C and then dramatically decreases by

Table 2
Corrosion parameters of the carbon films coated on 316L stainless steel in 1 M H_2SO_4 solution with 5 ppm F^- at 70 °C.

Substrate temperature (°C)	I_{corr} ($\times 10^{-8}$ A cm^{-2})	E_{corr} (mV vs. SCE)
100	6.4	+268
200	5.6	+329
300	14	+354
400	16	+173
500	64	+110
500[a]	43	+97

[a] Sample that cooled slowly after deposition.

increasing the substrate temperature. E_{corr} increase is related to the cathodic reactions in corrosion which is hydrogen gas evaluation as a predominant reaction in acidic solutions. In other words increasing the exchange current density (i_0) can increase the corrosion potential. One of the most important parameters that affects i_0 is surface morphology and roughness [27]. Increasing substrate temperature can modify the grain size of graphite crystallites, defects, and roughness. Dramatic decrease in corrosion potential at temperatures higher than 300 °C is related to the anodic reactions that are mainly originating from corrosion of substrate. When substrate is exposed to corrosion solution, the anodic reaction will increase. This phenomenon is shown in Fig. 5. Corrosion rate (i_{corr}) is relatively low and nearly constant up to 300 °C and then is increased by raising the deposition temperature. Fig. 6 shows SEM micrographs of carbon coating at 200 and 400 °C. Comparing two images, we observe that the pine-hole density has been increased and the cracks are formed on the surface of deposited film at 400 °C (shown by arrows).

Therefore, it seems that surface defects are created at high temperature results in high corrosion rate. The defects may be related to the thermal stress during the sample cooling after deposition. It means the defects are the consequence of thermal expansion coefficient difference between 316L stainless steel and carbon film. The conventional cooling rate of the samples is about 4.8 °C min^{-1}. However, by reducing the cooling rate to 15.8 °C min^{-1} (decrease more than three times), the corrosion rate does not decrease significantly (Table 1).

A similar dependence between carbon film porosity and substrate temperature has been reported by Mounier et al. [28].

From Fig. 6a one observes that, amorphous carbon films (a-C) deposited at low temperatures are relatively dense and without porosity. If one considers the constant flux of carbon atoms arriving at the surface of substrate, it is expected that the increase

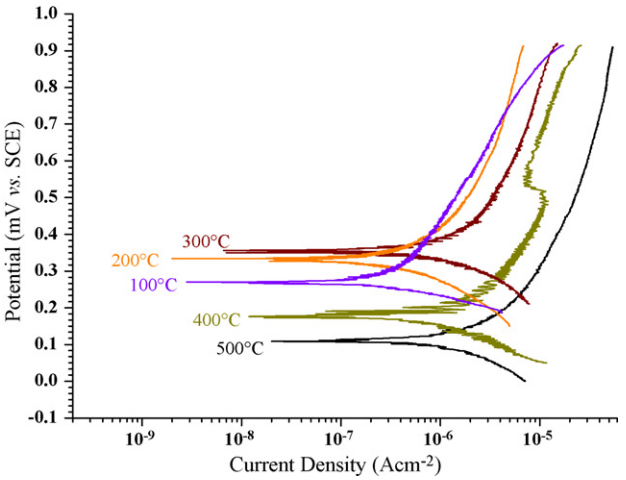

Fig. 4. Potentiodynamic curves of carbon films deposited at various temperatures in1 M H_2SO_4 solution with 5 ppm F^- at 70 °C.

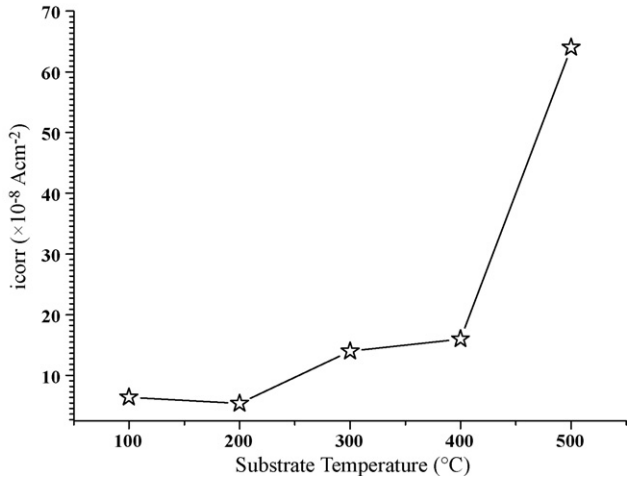

Fig. 5. Dependence of corrosion current density (I_{corr}) of carbon films on substrate temperature.

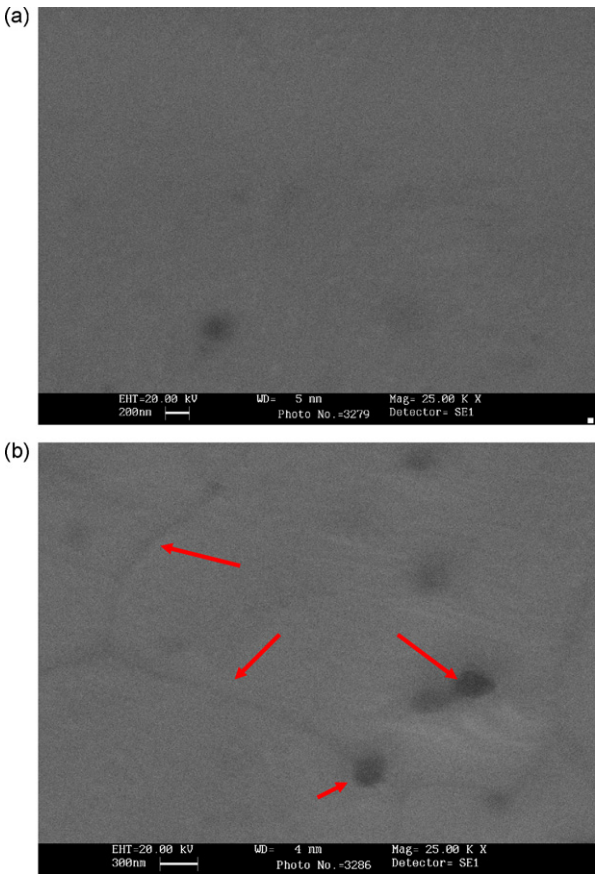

Fig. 6. SEM micrograph of the carbon film surface deposited at (a) 200 °C and (b) 400 °C. The scales are 200 and 300 nm for (a) and (b), respectively.

of temperature results in increasing of the mass density due to the graphitization. However, in consistent with our observation in Fig. 6b, Mounier et al. [28], indicated a reduction of carbon film mass density by increasing the temperature too, probably because of porosity increments.

In accordance with some investigations [6,10,14], the corrosion current density less than 16 $\mu A\,cm^{-2}$ has been recommended for bipolar plates. It can be seen from Fig. 5 that, all of the samples were prepared at temperatures below 400 °C can satisfy the proposed recommendation.

In the real PEMFC working conditions, the anode and cathode potentials are at around −0.1 V vs. SCE and +0.6 V vs. SCE, respectively [8,14,29]. In our case, the anode potential of PEMFC for all carbon-coated samples is located in cathodic branch. Therefore it is expected that no corrosion will be appear in anode side of the carbon-coated 316L stainless steel bipolar plates. In other words, carbon films at anode potential are under cathodic protection. However, the condition for the cathode side is different, because cathode potential for all deposition temperatures is located in anodic branch of potentiodynamic curve. Thus, it seems that corrosion will happen in cathode side of the carbon-coated 316L stainless steel bipolar plates. It should be noted that the magnitude of corrosion is important. Therefore, complete tests under more practical conditions of PEMFC are necessary. It includes potentiostatic tests under hydrogen purge and measuring dissolved ions in solution by ICP method. Authors are going to do these experiments in feature.

The sheet resistivity (ρ) of films deducted from relation (1) at different substrate temperature is summarized in Table 3. Fig. 7 shows the sheet resistivity of the carbon films extracted from Table 3. As it can be seen, ρ decreases dramatically up to 300 °C, and remains constant above that. The similar trend has been reported in [15,21].

Table 3
Sheet resistivity of carbon films on 316L stainless steel as a function of substrate temperatures.

Substrate temperature (°C)	100	200	300	400	500
R_s (Ω)	2452.90	950.14	141.09	81.40	67.42
t (nm)	80.1	96.2	106.1	146.0	207.1
ρ (Ω cm)	89.60	41.28	6.63	5.15	6.02

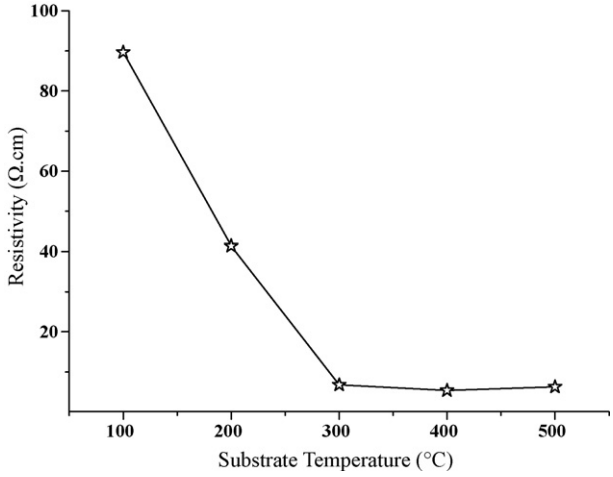

Fig. 7. The sheet resistivity of the carbon films deposited at various temperatures.

Show [15] has declared that, the deposited a-C film at room temperature presents a high resistivity above the detection limit of the four point-probe instrument. The decrease of resistivity is due to the graphitization of amorphous film by increasing substrate temperature as concluded from Raman results. It is worth to notice that at elevated temperatures (above 400 °C in our case) the quality of deposited film decreases by the formation of extended defects such as cracks and voids which lead to degradation of the film corrosion resistance. From the above discussion, it seems necessary to find a compromise between chemical and electrical properties of prepared films with choose of adequate substrate temperature. According to our results, it is inferred that working temperature of 300 °C can satisfy the mentioned request. Saturation of resistivity in elevated temperatures is a result of equilibrium between film graphitization and quality degradation.

4. Conclusion

The carbon was coated on 316L stainless steel by flat DC MS-PVD at different substrate temperatures was changed from 100 to 500 °C. The results show that in temperatures less than 300 °C, the films present an amorphous structure however, in temperatures higher than 300 °C, the fine-grained graphite (from 1.34 to 1.57 nm) forms and the graphitization of the deposited films take place. At temperatures below 400 °C, films show a high corrosion resistance, but at higher temperatures it is decreased due to the degradation of the deposited film quality by formation of the cracks and porosities. Also, the electrical resistivity sharply decreases by temperatures rising up to 300 °C and then stabilizes above that temperature. To satisfy both chemical and electrical needs, an optimum value of substrate temperature is required that is 300 °C in our conditions.

References

[1] H. Tsuchiya, O. Kobayashi, Int. J. Hydrogen Energy 29 (2004) 985–990.
[2] J. Wind, R. Spah, W. Kaiser, G. Bohm, J. Power Sources 105 (2002) 256–260.
[3] A.-M. Lafront, E. Ghali, A.T. Morales, Electrochim. Acta 52 (2007) 5076–5085.
[4] S. Jin, E. Ghali, A.T. Morales, J. Power Sources 162 (2006) 294–301.

[5] E. Fleury, J. Jayaraj, Y.C. Kim, H.K. Seok, K.Y. Kim, K.B. Kim, J. Power Sources 159 (2006) 34–37.
[6] H. Tawfika, Y. Hung, D. Mahajan, J. Power Sources 163 (2007) 755–767.
[7] M.H. Oh, Y.S. Yoon, S.G. Park, Electrochim. Acta 50 (2004) 777–780.
[8] H. Wang, J.A. Turner, J. Power Sources 128 (2004) 193–200.
[9] H. Wang, M.A. Sweikart, J.A. Turner, J. Power Sources 115 (2003) 243–251.
[10] A. Hermann, T. Chaudhuri, P. Spagnol, Int. J. Hydrogen Energy 30 (2005) 1297–1302.
[11] V.V. Nikam, R.G. Reddy, Electrochim. Acta 51 (2006) 6338–6345.
[12] D.P. Davies, P.L. Adcock, M. Turpin, S.J. Rowen, J. Appl. Electrochem. 30 (2000) 101–105.
[13] A. Pozio, R.F. Silva, M. De Francesco, L. Giorgi, Electrochim. Acta 48 (2003) 1543–1549.
[14] T. Fukutsuka, T. Yamaguchi, S.-I. Miyano, Y. Matsuo, Y. Sugie, Z. Ogumi, J. Power Sources 174 (2007) 199–205.
[15] Y. Show, Surf. Coat. Technol. 202 (2007) 1252–1255.
[16] Y. Show, M. Miki, T. Nakamura, Diam. Relat. Mater. 16 (2007) 1159–1161.
[17] C.-Y. Chung, S.-K. Chen, P.-J. Chiu, M.-H. Chang, T.-T. Hung, T.-H. Ko, J. Power Sources 176 (2008) 276–281.
[18] C.-Y. Chung, S.-K. Chen, T.-S. Chin, T.-H. Ko, S.-W. Lin, W.-M. Chang, S.-N. Hsiao, J. Power Sources 186 (2009) 393–398.
[19] Y. Fu, G. Lin, M. Hou, B. Wu, Z. Shao, B. Yi, Int. J. Hydrogen Energy 34 (2009) 405–409.
[20] K. Feng, Y. Shen, H. Sun, D. Liu, Q. An, X. Cai, P.K. Chu, Int. J. Hydrogen Energy 34 (2009) 6771–6777.
[21] A.A. Onoprienko, V.V. Artamonov, I.B. Yanchuk, Surf. Coat. Technol. 172 (2003) 189–193.
[22] E. Cappelli, S. Orlando, G. Mattei, S. Zoffolti, P. Ascarelli, Appl. Surf. Sci. 197–198 (2002) 452–457.
[23] M.A. Capano, N.T. McDevitt, R.K. Singh, F. Qian, J. Vac. Sci. Technol. A 14 (1996) 431–435.
[24] D. Beeman, J. Silverman, R. Lynds, M.R. Anderson, Phys. Rev. B 30 (1984) 870–875.
[25] J. Robertson, Mater. Sci. Eng. R37 (2002) 129–281.
[26] A.C. Ferrari, J. Robertson, Phys. Rev. B 61 (2000) 14095–14107.
[27] M.G. Fontana, Corrosion Engineering, 3rd edition, McGraw-Hill, 1986, ISBN 9780070214637.
[28] E. Mounier, F. Bertin, M. Adamik, Y. Pauleau, P.B. Barna, Diam. Relat. Mater. 5 (1996) 1509–1515.
[29] M. Kumagai, S.-T. Myungb, R. Asaishib, Y. Katadac, H. Yashirob, J. Power Sources 185 (2008) 815–821.